

# Layer-by-Layer Deposited Titanate-Based Nanotubes for Solar Photocatalytic Removal of Chemical Warfare Agents from Textiles\*\*

Mathieu Grandcolas, Alain Louvet, Nicolas Keller, and Valérie Keller\*

Since the discovery of carbon nanotubes by Iijima,<sup>[1]</sup> extensive research on the synthesis of nanotubes made of materials other than carbon, and especially of oxides such as  $\text{MoO}_3$ ,  $\text{WO}_3$ ,  $\text{VO}_x$ , and  $\text{TiO}_2$  has been reported.<sup>[2]</sup> In recent years,  $\text{TiO}_2$  and materials derived from  $\text{TiO}_2$  have been the focus of numerous investigations for applications in photovoltaic cells,<sup>[3]</sup> gas sensors, ultraviolet blockers, and for promising applications in photocatalysis. Moreover, nanoscale one-dimensional  $\text{TiO}_2$  materials have recently attracted much attention,<sup>[4]</sup> as they offer a larger surface area available in comparison to nanoparticles and also provide channels for enhanced electron transfer.<sup>[4]</sup> The nanotubes have high adsorption capacity, and efficient charge separation can be achieved on their surfaces, which reduces the recombination of photogenerated electrons and holes<sup>[5]</sup> that play determining roles in photocatalytic reactions.

The threat from chemical warfare agents (CWAs) has evolved over the past century. Attacks both on the battlefield and in civilian areas have demonstrated the high occurrence of casualties and thus the need for efficient protection. Therefore, post-use decontamination procedures on exposed and contaminated materials are much required. The current methods investigated are incineration, destruction, and neutralization using various chemicals, adsorption of the contaminants by an adsorbant, and the use of impermeable membranes. All of these methods present significant drawbacks as they cannot be directly applied on the battlefield, or these methods do not lead to the destruction of the toxic agents, but rather the adsorption of or a skin barrier to the contaminants.

The photocatalytic activity of  $\text{TiO}_2$  has been widely studied ever since its photoactivity was discovered in 1972 by Fujishima and Honda.<sup>[6]</sup> The development of high aspect ratio  $\text{TiO}_2$  nanostructures with high efficiency for solar photocatalytic applications is one of the biggest challenges concerning this material. Herein, we report the first use of coupled  $\text{WO}_3$ /titanate nanotubes for efficient degradation of simulants and real chemical warfare agents (blistering and

nerve agents) under solar illumination. Efficient performance of the titanate nanotubes (TiNTs) for direct degradation of gas-phase agents has been observed. Furthermore, a layer-by-layer (LbL) deposition of TiNTs on textiles can provide additional protection against percutaneous exposure to toxic liquids, vapors, and aerosols.

Figure 1 and Figure 2 show transmission electron microscope (TEM) images of the one-dimensional  $\text{WO}_3$ /TiNTs at different steps of its synthesis. The titanate (Figure 1 a) was

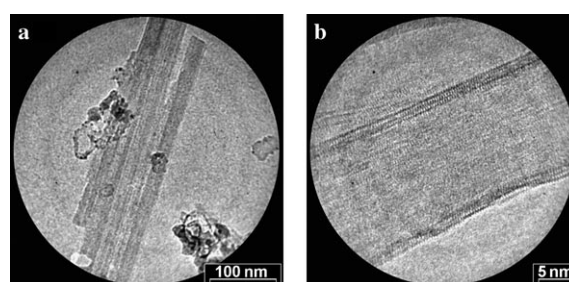


Figure 1. TEM image of a) raw titanate nanosheets and b) titanate nanotubes (TiNTs).

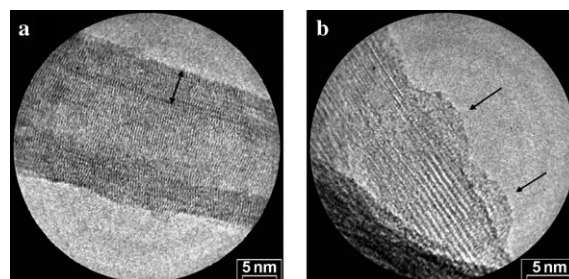


Figure 2. a) TEM and b) HRTEM images of  $\text{WO}_3$ /TiNT (4 wt. % of  $\text{WO}_3$ ) calcined at 380 °C.

first obtained as an aligned nanosheet, which upon washing with HCl until neutralization and drying at 110 °C led to open-ended TiNT tubes (Figure 1 b) with lengths of several tens or hundreds of nm and diameters around 15 nm and with a multilayered wall thickness of less than 2 nm. This is in agreement with the results reported in the literature.<sup>[7]</sup> As the temperature was increased to 380 °C to crystallize  $\text{WO}_3$  (Figure 2 a), following the impregnation of the TiNT tubes with the tungstate salt, the wall thickness of the TiNT tubes increased from 2 nm to almost 5 nm. The high magnification image (Figure 2 b) shows decoration of the TiNT with nanoscale islands of  $\text{WO}_3$  particles. The images of  $\text{WO}_3$ /TiNT (4 wt. % of  $\text{WO}_3$ , calcined at 380 °C) show that the tubular structure

[\*] M. Grandcolas, Dr. N. Keller, Dr. V. Keller  
LMSPC (Laboratoire des Matériaux, Surfaces et Procédés pour la Catalyse)—ELCASS (European Laboratory for Catalysis and Surface Sciences), CNRS, Louis Pasteur University  
25 rue Becquerel, 67087 Strasbourg (France)  
E-mail: vkeller@chimie.u-strasbg.fr

Dr. A. Louvet

DGA (Délégation Générale à l'Armement), CEB (Centre d'Etudes du Bouchet), 91710 Vert-le-Petit (France)

[\*\*] The authors thank DGA (Délégation Générale à l'Armement) for financial support. Dr. Corinne Ulhaq is thanked for TEM images.

remain and no agglomeration of particles located on the outer wall of the TiNT can be observed. The XRD pattern (Figure 3) of the material obtained directly after synthesis

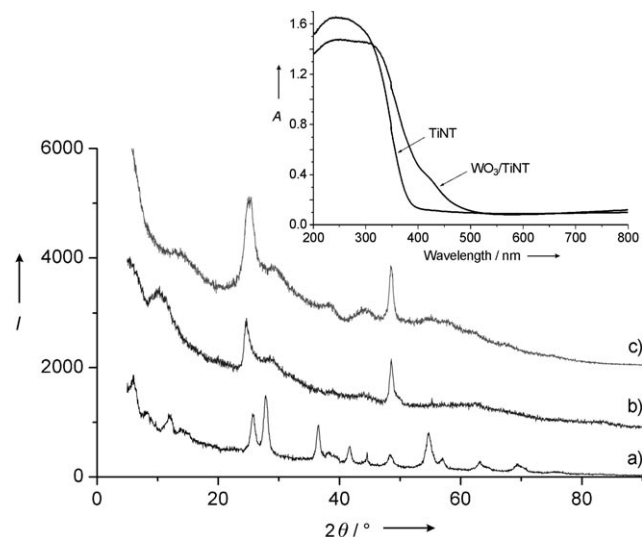


**Figure 3.** a,b,c) XRD patterns of the TiNTs. a) Crude titanates (TiNTs) synthesized by the hydrothermal method, b) after washing with HCl until neutralization and drying, c)  $\text{WO}_3/\text{TiNT}$  calcined at  $380^\circ\text{C}$ . Inset: UV/Vis absorption spectra of TiNT after acid washing and drying, and of  $\text{WO}_3/\text{TiNT}$ . For all the above cases, 4 wt. % of  $\text{WO}_3$  is present in  $\text{WO}_3/\text{TiNT}$ .

and without any treatment can be assigned to sodium titanate nanosheets of  $\text{Na}_2\text{Ti}_3\text{O}_7$  (Figure 3a).<sup>[8]</sup> After washing with HCl, this sodium-containing structure is transformed into another structure which could be indexed to  $(\text{Na}, \text{H}_2)/\text{Ti}_3\text{O}_7$  nanotubes (Figure 3b), or to  $\text{H}_2\text{Ti}_3\text{O}_7$  nanotubes according to literature.<sup>[9]</sup> This transformation results from interlayer exchange (partial or total) of cations ( $\text{Na}^+$  and  $\text{H}^+$ ), leading to bending and rolling of the nanosheets.

Impregnation with the tungstate salt followed by calcination at  $380^\circ\text{C}$  do not affect the XRD pattern of the washed and dried TiNT, with the exception of line broadening at low diffraction angles, which was attributed to an increase in the thickness of the walls. The resulting  $\text{WO}_3/\text{TiNT}$  exhibits high specific surface area of  $300\text{--}400\text{ m}^2\text{ g}^{-1}$ . UV/Vis absorption spectroscopy of the  $\text{WO}_3/\text{TiNT}$  material shows an absorption of the composite in the UVA and in the visible region of the spectrum (Figure 3 inset), suggesting the potential use of these nanocomposites under solar light irradiation conditions (UVA and visible-light wavelengths).

Continuous on-stream degradation of diethylsulfide (DES), which is considered a simulant for the yperite blistering agent (mustard gas, bis(2-chloroethyl)sulfide), using artificial solar light was performed on an annular concentric reactor<sup>[10]</sup> on  $\text{WO}_3/\text{TiNT}$  (Figure 4). It must be emphasized that calcined TiNT without  $\text{WO}_3$  exhibits poor solar photocatalytic activity. For comparison, pure  $\text{WO}_3$  and  $\text{WO}_3/\text{SiO}_2$  (more comparable with  $\text{WO}_3/\text{TiNT}$ ) showed no photocatalytic activity towards DES removal. The composite  $\text{WO}_3/\text{TiNT}$  used in all cases contained 4 wt. % of  $\text{WO}_3$ . The

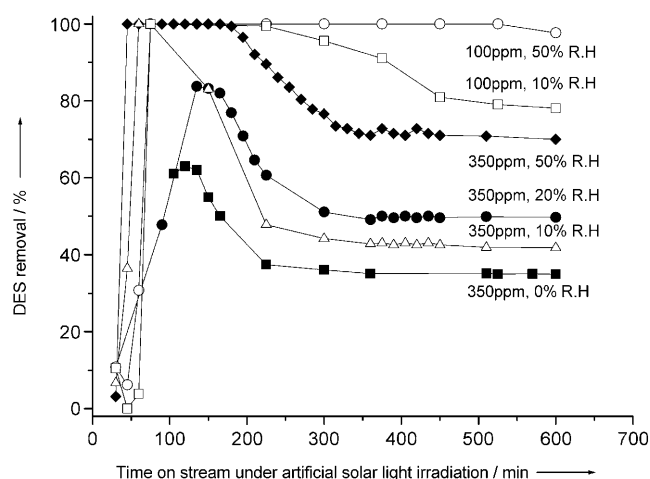


**Figure 4.** On-stream ( $50\text{ cm}^3\text{ min}^{-1}$ ) photocatalytic removal of diethylsulfide (DES) monitored at different DES concentrations and levels of relative humidity. Conditions: solar illumination 24 W, photocatalyst (440 mg) with  $1\text{ mg cm}^{-2}$  surface coverage of the reactor.

photocatalytic efficiency depends both on the relative humidity and on the initial concentration of DES; the lower the DES concentration, the higher the degradation efficiency, with little to no deactivation at a concentration of 100 ppm and at 50% relative humidity. Under these optimal experimental conditions, titanate nanotube-based materials ( $\text{WO}_3/\text{TiNT}$ ) exhibit immediate total degradation of the pollutant when exposed to solar illumination. Although the duration of total removal before deactivation depends on the humidity and pollutant concentration, the stabilized activity (reaching nearly 100% at low DES concentration) lasted several hours and thus was sufficient to ensure protection. It should be noted that 6 h is the standard maximum testing exposure delay for warfare agents according to standard NATO procedure. During the on-stream monitoring, other secondary organic products were also observed in the photocatalytic device. A complete study of gas-phase and surface intermediates will be published elsewhere.

This photocatalytic behavior can be further observed in the destruction or self-decontamination of clothing using  $\text{WO}_3/\text{TiNT}$ -based photocatalytic textiles. These active textiles can be obtained either by dip-coating, spray vaporization, or layer-by-layer (LbL) deposition. The LbL deposition method leads to deposition of homogeneous macro-scale and nano-scale tubular titanates on the micrometric textile fibers (Figure 5). This is the first time that titanate-based nanostructures have been deposited uniformly on a textile substrate using the LbL deposition method. The method offers the advantages of low-cost preparation with high-throughput layer fabrication, and results in a thin layer of material, as only material that bonds is deposited. These TiNT-based textiles have been investigated towards the detoxification of an organophosphonate simulant, dimethylmethylphosphonate (DMMP), and a blister agent, namely mustard gas. More precisely, following the NATO procedure tests,  $10\text{ g m}^{-2}$  of simulant or real warfare agents deposited as

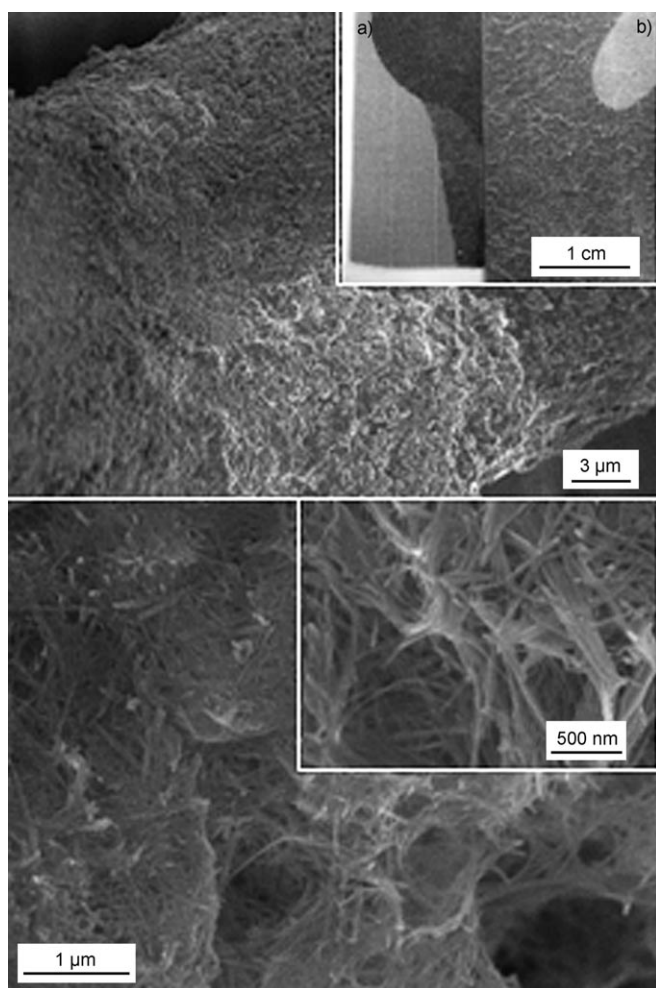


**Figure 5.** Views at different scales of cotton textile fibers coated with TiNT-based photocatalyst using the layer-by-layer (LbL) deposition. Inset a,b): a comparison between the a) LbL method and b) a classical spray deposition method.

droplets on the photocatalytic textile were illuminated using 24 W simulated solar light. Observed photocatalytic degradation was estimated after optimized extraction of the textile in an isopropanol solution and further quantification of the remaining extracted pollutant. The kinetics of degradation of DMMP as a function of illumination time is shown in Figure 6.

It is observed that natural DMMP removal occurs through DMMP evaporation during the exposure of the textile without the catalytic layer to solar light. In comparison, the optimized LbL-deposited textile shows efficient decontamination properties yielding total elimination of DMMP simulant within a few minutes (Figure 6). The removal of DMMP on photocatalytic textiles is not due to the super-hydrophilic properties enhancing the evaporation of DMMP, but due to photocatalytic degradation of the organic molecule. This has been ascertained by measuring the contact angles, which decrease during the illumination. Similar results have also been obtained for the yperite warfare agent.

In this work, we synthesized  $\text{WO}_3$ -titanate ( $\text{WO}_3/\text{TiNT}$ ) nanotube photocatalysts that can be easily and homogene-

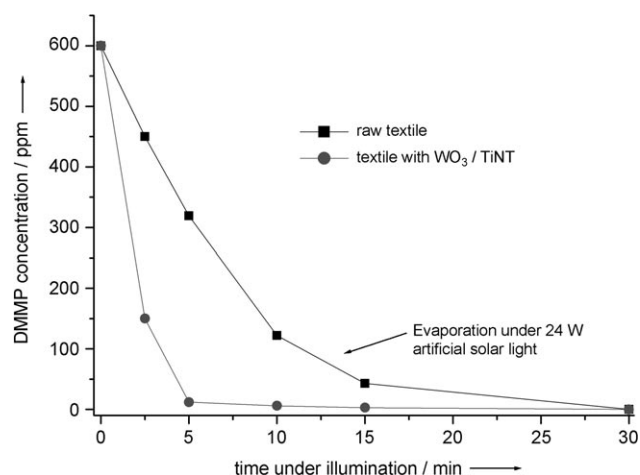


**Figure 6.** Kinetics of detoxification of contaminated TiNT-based textiles with DMMP simulant under artificial 24 W solar light illumination. 4 wt. % of  $\text{WO}_3$  is present in  $\text{WO}_3/\text{TiNT}$ .

ously coated onto textiles surfaces using LbL deposition. These titanates exhibit high oxidation performance in degrading nerve gas simulants and blister chemical agents under solar light illumination. The rapid and high photocatalytic activity can be attributed to the unique combination of physical and chemical properties of these one-dimensional materials. The nanotubular structure has a high surface area that is advantageous for an intimate  $\text{WO}_3/\text{TiNT}$  contact, leading to optimal titania- $\text{WO}_3$  semiconductor coupling. Owing to the lower band-gap (2.8–3.0 eV) of  $\text{WO}_3$ , a narrower bandgap semiconductor,  $\text{WO}_3/\text{TiNT}$ , is obtained that can absorb visible light. These one-dimensional photocatalytic materials can also be firmly and homogeneously deposited onto textile substrates, leading to new functionalized textiles.

In conclusion, it is possible to envisage protecting clothes that are not only based on impermeable or semipermeable barrier protection layers, but also on a permeable adsorptive protective overgarment, acting as an active destructive layer for the photochemical degradation of toxic chemicals.

## Experimental Section

Titanate nanotubes were synthesized by the hydrothermal treatment of  $\text{TiO}_2$  powder in concentrated  $\text{NaOH}$  solution (10 M) at 130 °C.<sup>[2c]</sup> In a typical synthesis,  $\text{TiO}_2$  powder (P25, Degussa; 1 g) was added to a  $\text{NaOH}$  solution (50 mL, 10 M) in a teflon autoclave, stirred for 1 h, and digested at 130 °C for 24 h. After the hydrothermal treatment, the white powder obtained was vacuum filtered and washed with  $\text{HCl}$  (2 M) and distilled water until the pH value was neutral followed by overnight drying at 110 °C. Coupled  $\text{WO}_3/\text{TiNT}$  was prepared by impregnating dried TiNT with ethanol/deionized water solution (1:3) of  $(\text{NH}_4)_{10}\text{W}_{12}\text{O}_{41}\cdot 5\text{H}_2\text{O}$  (W content: 1.6 g L<sup>-1</sup>). After stirring for 1 h, the mixture was sonicated before evaporating the solvent at room temperature for 24 h with constant stirring. The powder was dried and calcined for 2 h at 380 °C.

Layer-by-layer deposition was performed by the alternate immersion for 20 min of the textile substrate into either a polyethylenimine solution (8 g L<sup>-1</sup>) or a colloidal solution of  $\text{WO}_3$  (4 wt. %)/TiNT (pH 9, 10 g L<sup>-1</sup>). This sequence was repeated until the desired number of layers was attained. After deposition of each layer, the

substrate was rinsed three times with water. The final textile loaded with titanate nanotubes was then dried at 90 °C.

Received: June 29, 2008

Published online: November 26, 2008

**Keywords:** chemical warfare agents · photocatalysis · self-decontaminating textiles · titanium dioxide · tungsten oxide

- 
- [1] S. Iijima, *Nature* **1991**, 354, 56.
  - [2] a) Y. Feldman, E. Wasserman, D. A. Srolovitch, *Science* **1995**, 267, 222; b) M. Niederberger, H. J. Huhr, F. Krumeich, F. Bieri, D. Gunther, R. Nesper, *Chem. Mater.* **2000**, 12, 1995; c) T. Kasuga, M. Hiramatsu, A. Hoson, *Langmuir* **1998**, 14, 3160.
  - [3] a) M. R. Hoffmann, S. T. Martin, W. Choi, D. W. Bahnemann, *Chem. Rev.* **1995**, 95, 69; b) B. O'Regan, M. Graetzel, *Nature* **1991**, 353, 5358.
  - [4] a) Z. R. Tian, J. A. Voigt, J. Liu, B. McKenzie, H. Xu, *J. Am. Chem. Soc.* **2003**, 125, 12384; b) B. D. Yao, Y. F. Chan, X. Y. Zhang, W. F. Zhang, Z. Y. Yang, N. Wang, *Appl. Phys. Lett.* **2003**, 82, 281; c) T. Kasuga, M. Hiramatsu, A. Hoson, T. Sekino, K. Nihara, *Adv. Mater.* **1999**, 11, 1307.
  - [5] T. Tachikawa, S. Tojo, M. Fujitsuka, T. Sekino, T. Majima, *J. Phys. Chem. B* **2006**, 110, 14055.
  - [6] A. Fujishima, K. Honda, *Nature* **1972**, 238, 37.
  - [7] a) D. Bavykin, J. M. Friedrich, *Adv. Mater.* **2006**, 18, 2807; b) Q. Chen, W. Zhou, L. M. Peng, *Adv. Mater.* **2002**, 14, 1208.
  - [8] a) S. Andersson, *Acta Crystallogr.* **1962**, 15, 194; b) H. Izawa, S. Kikkawa, M. Koizumi, *J. Phys. Chem.* **1982**, 86, 5023.
  - [9] a) Q. Chen, G. H. Du, S. Zhang, L. M. Peng, *Acta Crystallogr. Sect. B* **2002**, 58, 587; b) Q. Chen, G. H. Du, R. C. Che, Z. Y. Yan, M. Peng, *Appl. Phys. Lett.* **2001**, 79, 3702.
  - [10] V. Keller, P. Bernhardt, F. Garin, *J. Catal.* **2003**, 215, 129.
-